The Importance of Kinetic and Thermodynamic Control when Assessing Mechanisms of Carboxylate-Assisted C-H Activation

The Importance of Kinetic and Thermodynamic Control when Assessing Mechanisms of Carboxylate-Assisted C–H Activation.

Raed A Alharis,[‡,a] Claire L. McMullin[†,b] David L. Davies,*[,a] Kuldip Singh,[a] and Stuart A. Macgregor.*[,b]

[a]Department of Chemistry, University of Leicester, Leicester, United Kingdom.

[b]Institute of Chemical Sciences, Heriot-Watt University, Edinburgh, United Kingdom, EH14 4AS.

KEYWORDS (Word Style "BG_Keywords"). If you are submitting your paper to a journal that requires keywords, provide significant keywords to aid the reader in literature retrieval.

ABSTRACT: The reactions of substituted 1-phenylpyrazoles (phpyz-H) at $[MCl_2Cp^*]_2$ dimers (M = Rh, Ir) in the presence of NaOAc to form cyclometalated Cp*M(phpyz)Cl have been studied experimentally and with DFT calculations. At room temperature, time-course and H/D exchange experiments indicate that product formation can be reversible or irreversible depending on the metal, the substituents and the reaction conditions. Competition experiments with both *para*- and *meta*-substituted ligands show that the kinetic selectivity favors electron donating substituents and correlates well with the Hammett parameter giving a negative slope consistent with a cationic transition state. However, surprisingly the thermodynamic selectivity is completely opposite with substrates with electron withdrawing groups being favored. These trends are reproduced with DFT calculations that show C–H activation proceeds by an AMLA/CMD mechanism. H/D exchange experiments with the *meta*-substituted ligands show *ortho*-C–H activation to be surprising facile, although (with the exception of F substituents) this does not generally lead to *ortho*-cyclometalated products. Calculations suggest that this can be attributed to the difficulty of HOAc loss after the C–H activation step due to steric effects in the 16e intermediate that would be formed. Our study highlights that the use of substituent effects to assign the mechanism of C–H activation in either stoichiometric or catalytic reactions may be misleading unless the energetics of the C–H cleavage step and any subsequent reactions are properly taken into account. The broader implications of our study for the assignment of C–H activation mechanisms are discussed.

Introduction

The use of carboxylate salts, particularly acetate and pivalate, to effect stoichiometric and catalytic C–H activation is now well established.[1-4] However several different terms are used to describe the mechanism of the C–H activation step, with, for aromatic substrates, S_EAr,[5] concerted metalation deprotonation (CMD),[6-8] ambiphilic metal ligand activation (AMLA)[9-10] and internal electrophilic substitution (IES)[11] being the most commonly cited. Electronic effects on reaction rates are often used to provide evidence to assign a particular C–H activation mechanism. For example, the observation of enhanced reactivity with more electron-rich substrates or with electron-donating substituents is often cited as evidence for an S_EAr process[12-16] or, if an internal base is involved, AMLA or BIES.[17-20] Alternatively, rate-enhancement with more electron-deficient substrates, or with more electron-withdrawing substituents, is often assigned to a CMD C–H activation mechanism.[21-25] We show here that such a strategy may be flawed unless a full understanding of the details of the C–H activation process under study are taken into account. Specifically, we will show below that the same cyclometalation reaction can give opposite substituent effects depending on whether the reaction is under kinetic or thermodynamic control. The implications of these observations in terms of distinguishing between S_EAr, AMLA, CMD and BIES are also discussed.

Early studies of substrate and substituent electronic effects on carboxylate-assisted C–H activation focused primarily on Pd. In the original experimental work by Ryabov on the cyclometalation of dimethylbenzylamines at $[Pd(OAc)_2]$ faster reactions were observed with electron donating groups on the phenyl being activated.[26] He proposed an S_EAr mechanism with deprotonation by a coordinated acetate ligand. Our 2005 computational study in fact showed the mechanism involved an agostic interaction of the C–H bond with the electron-deficient metal center with simultaneous H-bonding to the free oxygen of a metal-bound acetate.[10] These calculations also reproduced the substituent effects observed by Ryabov and we later termed this process Ambiphilic Metal Ligand Activation (AMLA).[9] More recently an ESI-MS study of the kinetics of C–H activation of substituted acetanilides by $[Pd(OAc]_2/CF_3CO_2H$ reached similar conclusions.[27]

In contrast, in 2006 both Maseras and Echavarren,[6] and Fagnou[7] independently showed that Pd-catalysed C–H activation could be favored by electron withdrawing groups. In their study, Maseras and Echavarren proposed a proton abstraction by a coordinated bicarbonate.[28] A very similar transition state with metal-bound bicarbonate was outlined by Fagnou for the direct arylation of fluorinated arenes. He termed these processes CMD, reflecting the *C*oncerted *M*etallation and C–H *D*eprotonation occurring in the transition state.[8]

These early results sometimes led to the conclusion that if electron rich substrates react faster it necessarily means that a CMD reaction cannot be in operation. However, Fagnou and Gorelsky subsequently showed that even electron rich (hetero) arenes that had previously been thought to favor an S_EAr mechanism actually react via CMD.[29-30] They rationalized the selectivity of C–H activation for a wide range of substrates using a distortion interaction analysis (Figure 1). Thus, π-electron rich arenes benefit from a large ΔE_{int} stabilization in the transition state which is offset by large destabilizing ΔE_{dist} values, while for electron-deficient arenes the complementary situation arises with lower ΔE_{int} and ΔE_{dist}.[29,31] In both scenarios the overall activation barrier, ΔE_{act}, is lowered relative to benzene. Based on the similarity of their transition states we have previously suggested that AMLA and CMD are essentially the same, in particular when the latter involves an internal base.[32]

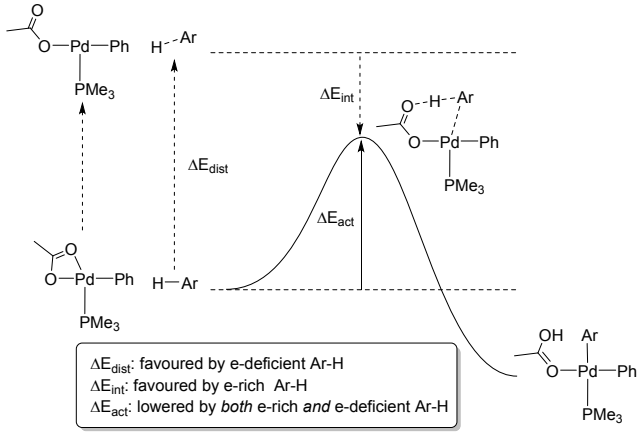

Figure 1. The distortion-interaction model applied to C–H activation of (hetero)aromatic substrates, Ar–H, at [Pd(OAc)Ph(PMe_3)]. Adapted from reference [29].

A later study by Ess suggested that the selectivity determining factor is the relative strength of the Pd–C bond being formed, the product with the stronger Pd–C bond being favored both kinetically and thermodynamically.[33] In contrast, Fairlamb et al. have recently shown that the regioselectivity of the cyclometalations of fluorinated dimethylbenzylamines at Pd is dependent on the Pd precursor used.[34] Thus, with [$Pd(OAc)_2$] roughly equal amounts of the *ortho* and *para* products are formed, whereas Li_2PdCl_4 gave exclusively the *para* isomer. Both reactions were proposed to be under kinetic control, with the former suggested to proceed via an AMLA/CMD mechanism, and the latter more likely via S_EAr.

Carboxylate-assisted C–H activation has subsequently been characterized at a range of different metals, including Rh and Ir.[1-4] However, despite the now widely established applications of such reactions in synthesis and catalysis there are surprisingly few detailed studies of electronic and steric effects on carboxylate-assisted C–H activation at these centers. Our original computational study on the cyclometalation of dimethylbenzylamine at [$IrCl_2Cp^*]_2$ in the presence of NaOAc[35] suggested an electrophilic activation with involvement of acetate as an intramolecular base, i.e. what we later[9] called an AMLA mechanism. This process requires an unsaturated, electron-deficient, i.e. "electrophilic", metal center; however, our literal use of this term has led to this process being interpreted as an S_EAr mechanism.[36, 37]

In 2008 Jones carried out an experimental study of the cyclometalation of phenylimines and phenylpyridines at [$MCl_2Cp^*]_2$ dimers (Scheme 1) and showed faster reactions for p-OMe-substituted over the p-CF_3-substituted ligands, and that Ir reacts faster than Rh.[36] For *meta*-substituted ligands steric factors led to a preference for the *para* isomer in the products. However there was no discussion as to whether these selectivities were kinetic and/or thermodynamic in origin.

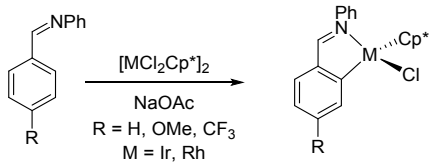

Scheme 1. Formation of cyclometalated imines.[36]

Later computational studies by Zhang et al. on this system suggested that C–H activation proceeded via an AMLA/CMD pathway with reaction being favored both kinetically and thermodynamically at Ir over Rh.[38] This agreed with the Ir reactions being faster experimentally but the higher activation energies for Rh were inconsistent with the reversibility of the reactions often seen at that metal. For example, we subsequently used H/D exchange experiments to demonstrate the reversible cyclometalation of N-phenylbenzaldimine at [$RhCl_2Cp^*]_2$ whereas no exchange is seen with [$IrCl_2Cp^*]_2$.[39] In this case computation gives similar activation barriers of around 18 kcal/mol at both Rh and Ir, with cyclometalation at Ir being significantly more exergonic. This was consistent with the cyclometalation of a range of hetero-aromatic imines being irreversible and so operating with kinetic selectivity at Ir. In contrast, these reactions at Rh were only slightly exergonic, consistent with their observed reversibility and leading to thermodynamic selectivity. Similar considerations may be relevant in the 2013 study by Müller et al. on the acetate-assisted cyclometalation of phosphinine ligands.[37] Faster reactions were initially seen with ligands featuring electron donating groups, leading to an S_EAr mechanism being proposed via an arenium ion intermediate. However, over longer time periods cyclometalation of an unsubstituted phenyl became favored over an OMe-substituted one.

Studies of Cp*Rh-catalysed C–H functionalization have often shown conflicting selectivity in terms of electronic effects with many reactions favoring electron donating groups,[12,14-16,18,40-44] whilst others favor electron with drawing groups.[21-22,45] For example, the catalytic C–H functionalisation of benzamides with Rh catalysts is promoted by substrates with electron withdrawing groups,[45] whereas in indole synthesis[46] substrates with electron donating groups react faster. Substituent effects may also impact on more than just the C–H bond cleavage step. For example, Frasco et al. showed computed barriers for the C–H activation of substituted benzenes at [$Ir(OAc)_2(DMSO)Cp^*$] correlated with the Hammett parameter for electron donating groups, but that no correlation was seen with electron withdrawing groups.[47] This is proposed to reflect the reversible formation of a H-bonded adduct prior to the C–H cleavage step, with electron withdrawing groups affecting more the energy of adduct formation, whilst electron-donating groups impact on the actual C–H bond cleavage step. Larrosa and Macgregor have

also shown that an holistic assessment of substituent effects is required to understand reactivity patterns in the Ru(II)-catalysed arylation of substituted benzoates, with benzoate binding, cyclometalation, and subsequent deprotonation of the benzoic acid formed, all contributing.[48]

In summary, several different mechanisms have been proposed for carboxylate-assisted C–H activation, including S_EAr, AMLA/CMD and BIES, and substituent effects have often been used to try to delineate these possibilities. In this study we investigate electronic and steric effects on the acetate-assisted cyclometalation of substituted 1-phenylpyrazoles at $[MCl_2Cp^*]_2$ dimers (M = Ir, Rh). We aim to characterize the mechanism of C–H activation and to explain the origin of the observed selectivities and find that a full appreciation of both kinetic and thermodynamic effects is essential if appropriate conclusions are to be drawn. We also consider the wider implications for mechanisms of carboxylate-assisted C–H activation. In particular what differences, if any, there are, between S_EAr, AMLA/CMD and BIES and whether electronic effects can be a good guide to distinguish between them?

Results and Discussion

Reactions of the *para*-substituted ligands (**L1-R**) with the appropriate dimer, $[MCl_2Cp^*]_2$, (M = Ir, Rh) in MeOH or a mixture of DCM and MeOH in the presence of NaOAc gave the *meta*-substituted compounds **1a-R** and **1b-R** respectively (Scheme 2). Similar reactions with *meta*-substituted ligands **L2-R** can, in principle, give rise to *ortho*- or *para*-substituted products (**2-R** and **3-R** respectively Scheme 3). All the compounds were fully characterized by ^1H and ^{13}C NMR spectroscopy and in several cases by X-ray crystallography (See SI). Compounds with **L1-H** have been reported previously.[49]

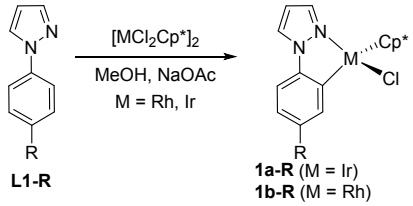

Scheme 2. Formation of *meta*-substituted cyclometalated complexes **1a-R** (M = Ir) and **1b-R** (M = Rh).

All of the reactions with $[IrCl_2Cp^*]_2$, went to > 90% conversion usually within 1 hour except for **L1-NO_2** which was slower. The corresponding reactions with $[RhCl_2Cp^*]_2$ were considerably slower and often did not go to completion. With electron withdrawing substituents the reactions required at least 24 hours to give conversions of >80% and for **L1-NO_2** the reaction required heating to 60 °C for high conversion (>90%). Jones has previously noted that cyclometalation reactions with $[RhCl_2Cp^*]_2$ often do not go to completion but reach equilibrium.[36]

For reactions with **L2-R** the isomer ratios for both metals are shown in Table 1. With the largest substituents (NMe_2 and CF_3) only the *para* isomers **3** were isolated for both Ir and Rh. In the reactions with **L2-Me**, Ir gave a small amount of the *ortho* isomer **2a-Me** whereas with Rh only the *para* isomer **3b-Me** was observed. The ligands with the more electronegative substituents **L2-OMe**, **-F** and **-NO_2** all showed a mixture of both isomers with both Ir and Rh. For **L2-F** in Table 1 the *ortho* isomer **2-F** is favored by Ir and Rh and in the case of Rh over time the preference for the *ortho* isomer increases.

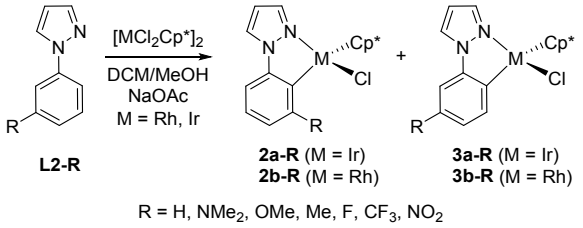

Scheme 3. Formation of *ortho* and/or *para*-substituted cyclometalated complexes **2a-R** and **3a-R** (M = Ir) and **2b-R** and **3b-R** (M = Rh).

Table 1. *ortho:para* ratios (**2-R**:**3-R)** for Ir and Rh complexes.

R	Ir		Rh	
	Initial ratio *o:p*	**Final ratio *o:p***	**Initial ratio *o:p***	**Final ratio *o:p***
NMe_2	0:1		0:1	
CF_3	0:1		0:1	
Me	1:10	1:10[a]	0:1	
OMe	1.2:1	1:1.4[c]	1:1.3 (1:4.2)[b]	1:3.9[c]
F	4.5:1	40:1[d]	19:1 (33:1)[b]	44:1[c]
NO_2	1:2.6	0:1[d]	2:1 (1:2.7)[b]	0:1[c]

[a] No significant change after heating but accurate integration difficult due to closeness of signals for both isomers. [b]Number in brackets is the ratio after several hours if there is a significant change at rt. [c]At 50 °C in MeOH/DCM mixture after several days heating. [d]In TFE with PivOH at 90 °C using excess ligand.

Overall, the results in Table 1 are consistent with previous observations that a bulky group favors the *para* isomer due to steric effects.[36] However, an important additional observation in our study is that in the reactions with Rh the ratio of isomers changed over time: for **L2-F** the *o:p* ratio increased from 19:1 to >30:1; with **L2-OMe** an initial *o:p* ratio of 1:1.3 increased to 1:4.2; and with **L2-NO_2** an initial *o:p* ratio of 2:1 (6% conversion) changed to 1:2.7 (55% conversion). These changes are consistent with the Rh reactions being reversible and that in all cases, except F, the *para* isomer is favored thermodynamically. In contrast, for the reactions with Ir none of the isomer ratios changed at room temperature. To investigate the thermodynamic selectivity further, the reactions were heated and in some cases pivalic acid was added to aid reversibility (Table 1, footnotes b and c). The results confirm that (again with the exception of **L2-F**) the *para* isomer is favored thermodynamically for both metals.

Several of the cyclometalated products were suitable for X-ray diffraction and the structures all show the expected piano stool geometry with the Cp* ring bonded asymmetrically to the metal center with two long M—C bonds (*trans* to the cyclometalated bond, M—C(9)) and three short ones (see Table S1a-c for structures and selected bond lengths and angles). For the meta-substituted complexes, **1-R**, there is no correlation between the M—C(9) bond length and the electron donating or withdrawing character of the substituent. For example, for Rh complexes **1b-NMe_2**, and **1b-CF_3** the Rh—C(9) distances [2.031(3) and 2.032(3) Å respectively] are statistically the same. Similarly for the *para*-substituted complexes **3b-OMe**, **3b-CF_3** and **3b-NO_2**, there is no

significant variation in Rh—C(9) bond length [2.049(3) Å **3b-OMe**, 2.026(8) Å **3b-CF$_3$** and 2.039(4) Å **3b-NO$_2$**]

Deuteration experiments

To check the reversibility of the reactions deuteration experiments were carried out (see Table S2). For ligands **L1-R** reacting at Ir there was no evidence for deuterium incorporation at room temperature, although **L1-NMe$_2$** did show H/D exchange (about 10% D) after heating at 50 °C for 3 days. In contrast, with Rh both **L1-NMe$_2$** and **L1-OMe** showed some deuterium incorporation even at room temperature (8% D after 2 days and 22% D after 10 days respectively). These results confirm that for Rh the C–H activation, with electron donating substituents, is reversible.

Similar deuteration experiments were also performed at room temperature for some[50] of the *meta*-substituted **L2-R** ligands. In this case, deuterium incorporation can, in principle, occur at two different positions, site A, *ortho* to the substituent and site B, *para* to the substituent (see Scheme 4 and Table S2).

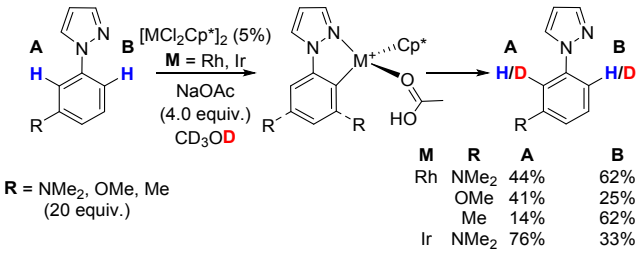

Scheme 4. Room temperature H/D exchange for *meta*-substituted ligands at sites A and B.

For Ir, only **L2-NMe$_2$** showed H/D exchange with 76% deuteration in position A and 33% in position B after just 15 minutes. Whilst exchange at position B is consistent with observation of the *para* product **3a-NMe$_2$**, exchange at position A is unexpected since it would correspond to formation of the *ortho* isomer **2a-NMe$_2$**, which was not observed as a product in the preparative reaction (see above). Indeed, the higher percentage exchange in site A compared to site B suggests that C–H activation at the *ortho* position is easier than at the *para* position which is opposite to what was expected on the basis of the observed cyclometalated products. Reaction of **L2-NMe$_2$** with Rh gave deuterium incorporation in both positions after 15 min (44% A 62% B), indicating that *ortho*-C–H activation is also feasible for Rh, athough exchange is faster in the *para* position in this case. For Rh, both **L2-OMe** and **L2-Me** showed H/D exchange at room temperature at both positions with site A favored for **L2-OMe** (41% A, 25% B) and site B favored for **L2-Me** (14% A, 62% B). These observations show C–H activation at the *ortho* position is accessible for Rh even though in the case of **L2-Me** no *ortho* product was observed in the preparative reaction.

Together, the deuteration studies and the changes in regioisomeric ratios indicate that C–H activation is more reversible with the electron donating substituents and that reactions with Rh are considerably more reversible than those with Ir. In addition, the lack of observation of the *ortho* isomer of the final cyclometalated product is not necessarily due to a higher barrier to C–H activation at that site.

Competition Experiments

Having prepared all the relevant complexes we then investigated their relative rates of formation by carrying out competition reactions in which two ligands compete for reaction with a limiting amount of metal (5:5:1 ratio of ligand:ligand:metal) (Scheme 5).

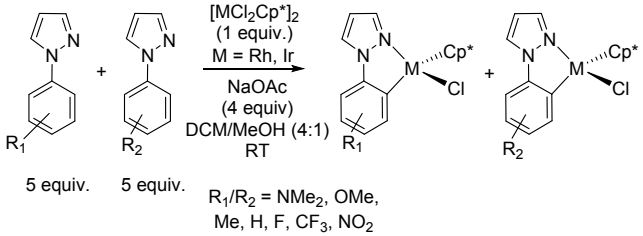

Scheme 5. Competition experiments; for results of individual experiments see ESI.

In initial experiments it was found that the reactions are much faster in MeOH than in DCM as has been observed previously for similar reactions.[36,39] However, some products were insoluble in pure MeOH hence the reactions were carried out in DCM:MeOH (4:1) to increase solubility and provide more convenient reaction times for monitoring by ^{1}H NMR spectroscopy. To establish whether any selectivity is kinetic or thermodynamic, the ratio of products was measured at room temperature after a short reaction time (usually 15 minutes) and again at longer times and after heating (if necessary, using TFE as a solvent in the presence of pivalic acid) to see if there was any change in the ratio.

The results of competition experiments of **L1-R** with $[IrCl_2Cp^*]_2$ in the presence of NaOAc to form *meta*-substituted complexes **1-R** are shown in Table S3, with those for **L2-R** in Table S4. For **L2-R**, to minimize overlap in the NMR spectra, where possible, competition reactions in which only one ligand would lead to two isomers were carried out.

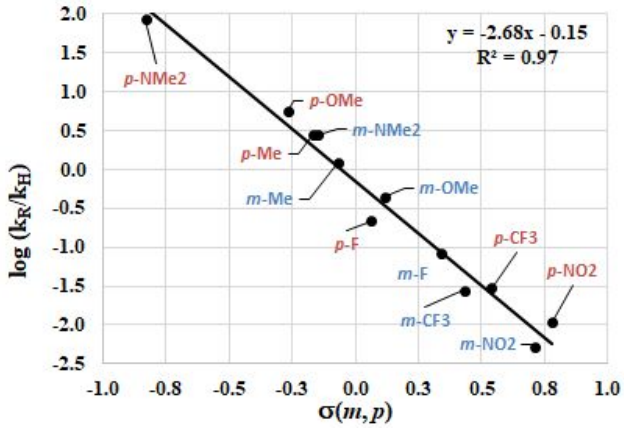

Figure 2. Hammett plot of log (k_R/k_H) for formation of *meta* **1-R** and *para*-substituted **3-R** complexes of Ir against σ_m and σ_p.

The relative rates of formation of the *meta*- and *para*-substituted complexes[51] are shown in Table S5 and the Hammett plot is shown in Figure 2. As can be seen, a good straight line (correlation = 0.97) with a negative slope (-2.7) was obtained when using σ_m and σ_p. The negative slope arises from faster reactions with electron donating substituents and is characteristic of a cationic intermediate with some build-up of positive charge in the transition state. However, the modest value (-2.7) for slope (ρ) is lower than expected for an S_EAr

mechanism.[5] In addition, a poorer fit (correlation = 0.89) with a negative slope (-1.7) was obtained when using σ_{m+} and σ_{p+} (see Figure S3) providing further evidence against an S_EAr mechanism.

The results of the competition experiments with $[RhCl_2Cp^*]_2$ are shown in the ESI (Tables S6 and S7) with the k_R/k_H values (Table S8) and the Hammett plot (Figure S4). The Hammett plot again shows a good straight line correlation (0.99) with a negative slope (-2.3). A poorer correlation (0.95) with a negative slope (-1.5) was obtained when using σ_m- and σ_{p+} (Figure S5).

As found for the *o*:*p* ratios described above, in the competition reactions, particularly for Rh and for electron donating substituents, the ratios of products changed over time (Tables S6 and S7). At short reaction times the ratio reflects kinetic selectivity and the later ones reflect the thermodynamic preference. For reactions with Ir and those with electron withdrawing substituents the reactions were heated, if necessary with pivalic acid to promote reversibility and hence achieve the thermodynamic selectivity The results are plotted as $\ln(K_R/K_H)$ (K_R/K_H = equilibrium ratio with respect to H) versus the Hammett parameter (Figure 3) and are discussed further below.

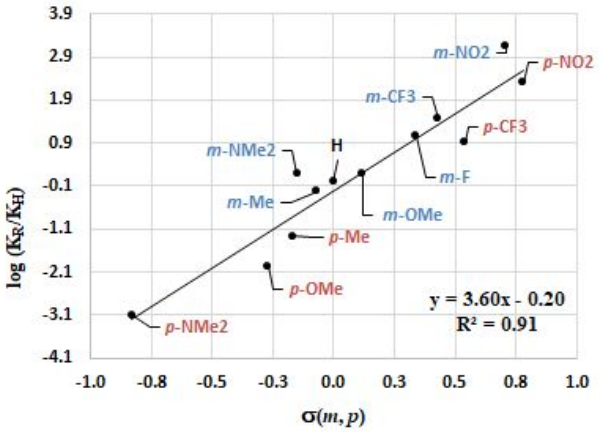

Figure 3. Plot of $\ln(K_R/K_H)$ for formation of *meta* **1a-R** and *para*-substituted **3a-R** complexes of Ir against σ_m and σ_p.

The plot shows a reasonable straight line with a positive slope showing that ligands with more positive Hammett values (i.e. with electron withdrawing substituents) now correlate with more thermodynamically stable products. This is entirely opposite to the kinetic selectivity. Thus, electron donating groups are favored kinetically but electron withdrawing groups are favored thermodynamically. It is clear therefore that if one were to draw conclusion about the type of mechanism involved on the basis of these electronic effects alone, a different answer would be obtained depending on whether the reaction were under kinetic or thermodynamic control. This also shows that a single mechanism can favor *either* electron donating groups *or* electron withdrawing groups based on the reaction conditions. We believe that this possibility has so far been overlooked.

Computational Studies

Kinetic and Thermodynamic Selectivities. To understand the different reactivity patterns exhibited by these $[MCl_2Cp^*]_2$ dimers, DFT calculations on the cyclometalation of ligands **L1-R** and **L2-R** have been carried out, using our previously established protocol[39] with DCM as solvent.[52] Computed profiles for the reactions of **L2-NMe$_2$** and **L2-NO$_2$** at $[IrCl_2Cp^*]_2$ and $[RhCl_2Cp^*]_2$ to give the *para*-substituted cyclometalated products, **3a-R** and **3b-R**, are shown in Figures 4a and 4b, respectively, along with the labelling scheme used in the computational study.

The computed mechanisms for these cyclometalation reactions are similar to those described previously by us[35,39,53] and others.[32] Opening the $[MCl_2Cp^*]_2$ dimers (**A**) with acetate produces both $[MCl(OAc)Cp^*]$ (**B**) and $[M(OAc)_2Cp^*]$ (**C**), and the energy of the latter (along with that of free **L2-NMe$_2$** or **L2-NO$_2$** as appropriate) is set to 0.0 kcal/mol. Ligand addition then forms $\mathbf{D}_p$, followed by loss of acetate to give cation $\mathbf{E}_p$. For **L2-NMe$_2$** C–H activation proceeds via an agostic intermediate, **Int(E-F)$_p$**,[54] and gives acetic acid adduct $\mathbf{F}_p$. Dissociative substitution of HOAc by Cl^- via $\mathbf{F1}_p$ then forms the final cyclometalated product $\mathbf{G}_p$. A similar sequence is seen with **L2-NO$_2$**, although in this case C–H activation occurs in a single step via **TS(E-F)$_p$**.[55]

The computed profiles show a clear kinetic preference for the reactions of **L2-NMe$_2$** at both Ir and Rh. For M = Ir the overall barrier is 15.6 kcal/mol with the rate-limiting transition state, $\mathbf{TS(E\text{-}F)1}_p$, corresponding to the κ^2-κ^1 displacement of acetate to form the agostic intermediate **Int(E-F)$_p$**. For M = Rh the C–H cleavage transition state, $\mathbf{TS(E\text{-}F)2}_p$ (+13.5 kcal/mol), is slightly higher than $\mathbf{TS(E\text{-}F)1}_p$ (+13.2 kcal/mol), although in this case 16e $\mathbf{F1}_p$ at +13.9 kcal/mol is actually the highest point on the profile. For **L2-NO$_2$** the highest lying stationary point, **TS(E-F)$_p$**, corresponds to similar barriers at both Ir (23.9 kcal/mol) and Rh (23.3 kcal/mol). Product formation with **L2-NO$_2$** is thermodynamically favored, with $\mathbf{G}_p$ being ca. 5 kcal/mol lower for **3-NO$_2$** than **3-NMe$_2$** for both metals.

To substantiate these trends, full reaction profiles were computed for the cyclometalation of the remaining **L2-R** ligands to form *para*-substituted complexes, as well as the full set of **L1-R** ligands to form the *meta*-substituted complexes **1a**/**1b-R** and full details of all these processes are provided in the ESI. In all these cases the highest lying stationary point is associated with the C–H activation process and plots of $\Delta G^‡$, the overall barrier, and ΔG, the overall free energy change to form the cyclometalated products, against the relevant σ_m and σ_p Hammett constants are shown in Figure 5(a) and 5(b) respectively. For both metals these show excellent, but opposite, correlations for $\Delta G^‡$ and ΔG, with electron donating groups providing lower barriers, and electron withdrawing groups greater reaction exergonicities. The calculations therefore capture the swap in the substituent effects seen experimentally when moving from kinetic to thermodynamic control. Computed values of $\Delta G^‡$ for Rh are consistently lower than for Ir, and this initially appears at odds with the faster cyclometalations seen at Ir. However, the lower reaction exergonicities at Rh suggest these processes will be more reversible (ΔG = -3 to -8 kcal mol^{-1}) than at Ir (ΔG = -7 to -14 kcal mol^{-1}). The longer reaction times at Rh therefore reflect a slow approach to equilibrium rather than a simple kinetic effect associated with the forward reaction. This is also consistent with some

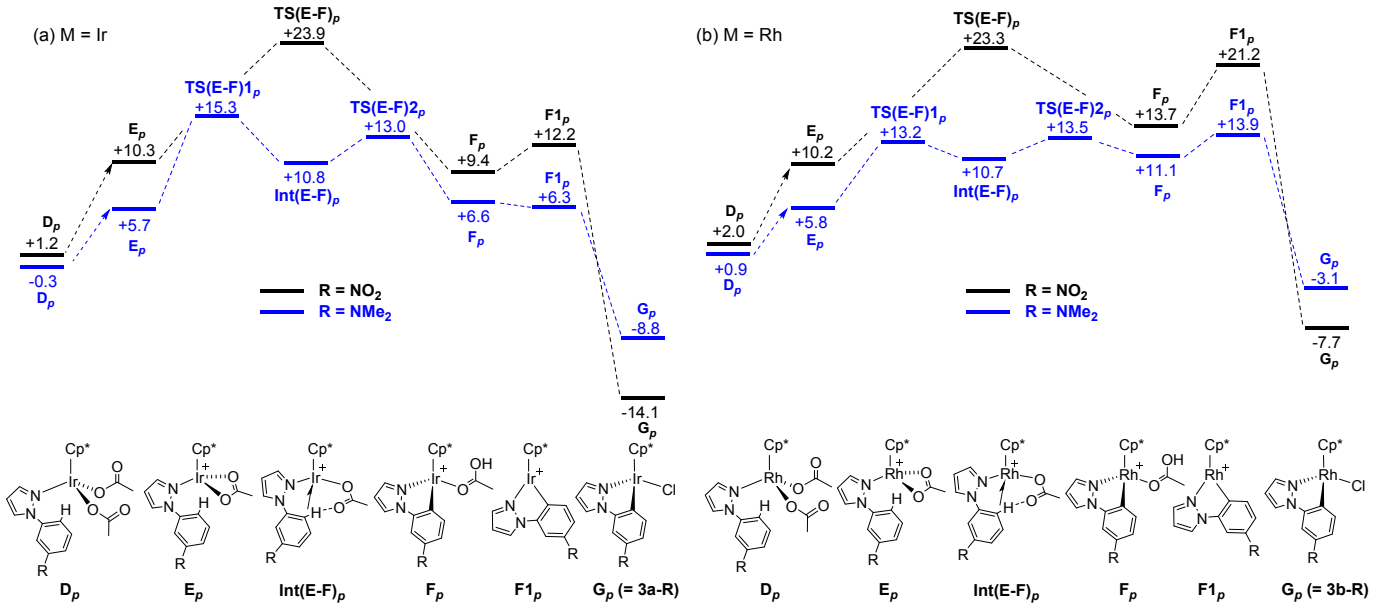

Figure 4. Computed free energy profiles (kcal/mol) for the reactions of **L2-NMe$_2$** (blue) and **L2-NO$_2$** (black) at (a) [IrCl$_2$Cp*]$_2$ and (b) [RhCl$_2$Cp*]$_2$. Free energies are quoted relative to [M(OAc)$_2$Cp*] (**C**) and the free ligand set to 0.0 kcal/mol.

of the Rh reactions not reaching completion (in particular with electron donating substituents for which ΔG is smallest), with the observed changes in *o:p* isomer ratios as several of these reactions proceed, as well as with the observation of H/D exchange mediated by Rh. For Ir the reaction with **L2-NMe$_2$** to give **3a-NMe$_2$** has the lowest barrier and is the least exergonic, and these features are consistent with this being the only reaction at Ir that is reversible at room temperature.

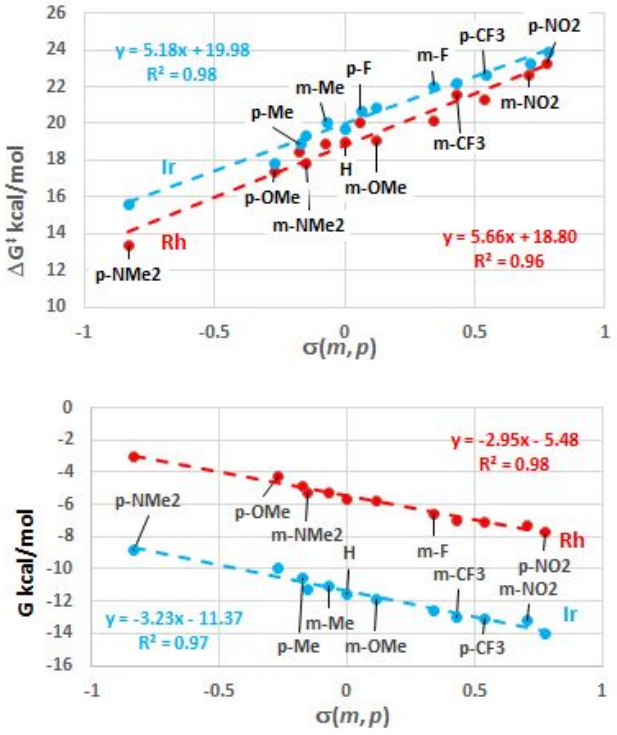

Figure. 5. Plots of computed values of ΔG‡ and ΔG (kcal/mol) against σ_m and σ_p Hammett constants for the reactions of **L1-R** and **L2-R** to form **1a/b-R** and **3a/b-R**.

***Ortho*-C-H Activation.** Calculations were also employed to account for the different *ortho*/*para* selectivities seen with the ligands **L2-R** (Table 1) and in particular the surprising observation of *ortho*-H/D exchange in the reactions of **L2-NMe$_2$**, **L2-Me** and **L2-OMe** at Rh, as well for **L2-NMe$_2$** at Ir (Scheme 4). Figure 6 compares computed pathways for *ortho*- and *para*-cyclometalation of **L2-NMe$_2$**, **L2-Me**, **L2-OMe** and **L2-F** at Rh, where the profiles have been truncated to show just the highest lying transition state prior to the formation of the C–H activated intermediates **F$_{o/p}$** as well as their onward reactions via **F1$_{o/p}$** to form the products **G$_{o/p}$**.

Experimentally for Rh both **L2-NMe$_2$** and **L2-Me** form exclusively the *para*-substituted products and the computed profiles are consistent with this with the *para*-pathways (in blue) exhibiting lower overall barriers and the *para*-substituted products being more stable. The *ortho*-pathways (in red) actually have similar barriers for the formation of **F$_o$**, however the high energy of 16e **F1$_o$** means the *ortho*-pathway is kinetically disfavored. The reactions of **L2-F** and **L2-OMe** show *o/p* mixtures at room temperature with final ratios of 44:1 and 1:3.9 respectively. For **L2-F** formation of the *ortho*-product is computed to be favored kinetically and thermodynamically, consistent with the observed *ortho*-selectivity. A similar pattern is computed with **L2-OMe** and suggests the *ortho*-isomer should again dominate; experimentally a final *o:p* ratio of 1:3.9 is seen, which indicates the two products must be very close in energy. In contrast to **L2-NMe$_2$** and **L2-Me**, for both **L2-F** and **L2-OMe** intermediate **F1$_o$** lies below the preceding C–H activation transition state.

The high energies of intermediates **F1$_o$** computed with **L2-NMe$_2$** and **L2-Me** arise from the proximity of the *ortho* substituent to the Cp* ring (see Figure 7 for **L2-NMe$_2$**). This results in structural distortion, as seen in the angle between the best-fit planes of the Cp* C$_5$ ring and the {RhNNCC} metallacycle (67.7°), as well as in the sp^3-hydridisation of the NMe$_2$

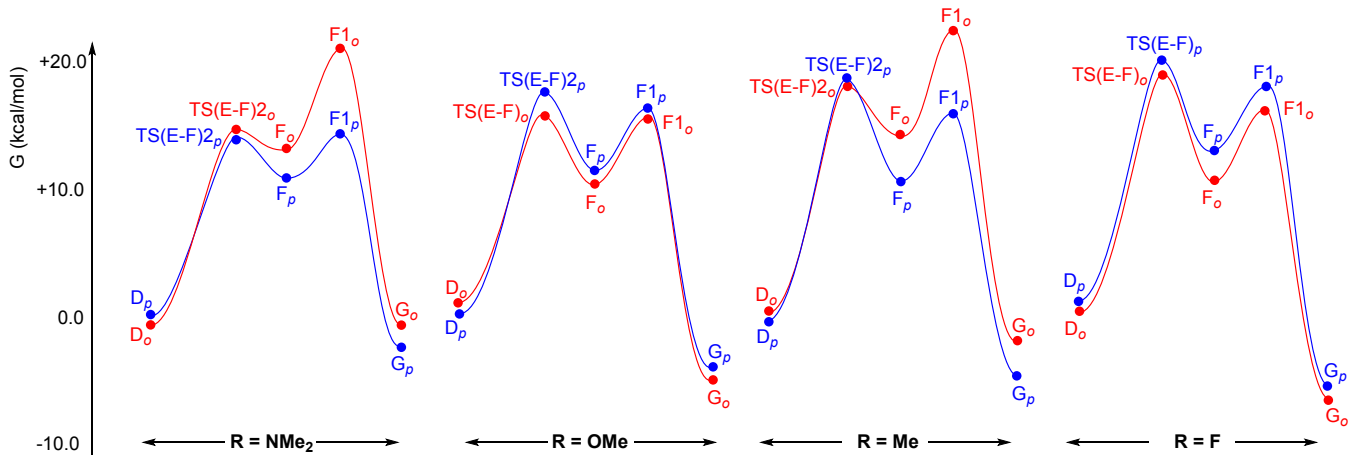

Figure 6. Computed free energy profiles (kcal/mol) for the *ortho*- (red) and *para*-cyclometalation reactions (blue) of **L2-R** at $[Rh(OAc)_2Cp^*]$.

nitrogen (sum of angles around N = 342.5°) that serves to reduce the steric clash with the Cp* ring. In contrast, in the absence of steric effects, $\mathbf{F1}_p$ displays effective C_s symmetry.

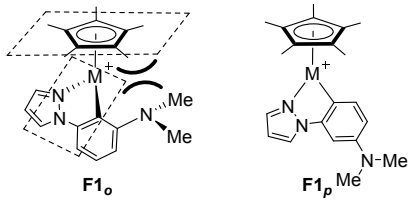

Figure 7. Schematic structures of $\mathbf{F1}_o$ and $\mathbf{F1}_p$ illustrating steric hindrance in $\mathbf{F1}_o$.

Significantly, Figure 6 shows the steric effect associated with the *ortho*-Me and NMe_2 substituents only begins to have a major energetic impact once the M–C bond has been formed in $\mathbf{F}_o$, and this presumably reflects the greater distances between the *ortho* substituent and the Cp* ring prior to that point. *ortho*-C-H activation to form HOAc adduct $\mathbf{F}_o$ is therefore readily accessible for both **L2-Me** and **L2-NMe$_2$** even if the onward reaction to form $\mathbf{G}_o$ is then disfavored. *ortho*-deuteration of the free ligand can be accounted for via reversible formation of $\mathbf{F}_o$, with H/D exchange with CD_3OD co-solvent occurring at $\mathbf{F}_o$. With **L2-OMe** H/D exchange could in principle also occur at $\mathbf{F}_o$, but in this case onward reaction to form $\mathbf{G}_o$ is accessible and reversible. HOAc can therefore undergo H/D exchange with CD_3OD solvent before reacting with $\mathbf{G}_o$ to deuterate the ligand. Of the remaining **L2-R** ligands, **L2-CF$_3$** behaves in a similar way to **L2-NMe$_2$**/**L2-Me** while **L2-NO$_2$** is more like **L2-F**/**L2-OMe**. With **L2-NO$_2$** the *ortho*-pathway is computed to be favored kinetically while the *para*-substituted cyclometalated product is more stable, and these results are consistent with the evolution of the *o*:*p* ratio seen experimentally, from initially a 2:1 ratio to 1:10 over longer timescales.

Computed profiles for the reactions of **L2-NMe$_2$** at Ir are shown in Figure 8. Formation of $\mathbf{F}_o$ can readily occur via $\mathbf{TS(E\text{-}F)1}_o$ and the subsequent loss of HOAc again entails an additional energetic cost. This effect is, however, less significant than for the Rh systems and as a consequence $\mathbf{F1}_o$ is similar in energy to $\mathbf{TS(E\text{-}F)1}_p$, the high point along the *para* pathway. Experimentally, H/D exchange indicates both the *ortho*- and *para*-reactions are reversible and so the observed product will be formed under thermodynamic control, and computationally, $\mathbf{G}_p$ is found to be 1.7 kcal/mol more stable than $\mathbf{G}_o$. Moreover, H/D exchange with CD_3OD solvent could occur at $\mathbf{F}_o$ or upon dissociation of HOAc in forming $\mathbf{F1}_o$ or $\mathbf{G}_o$, the reversibility of all these processes allowing for *ortho*-H/D exchange at the free ligand.

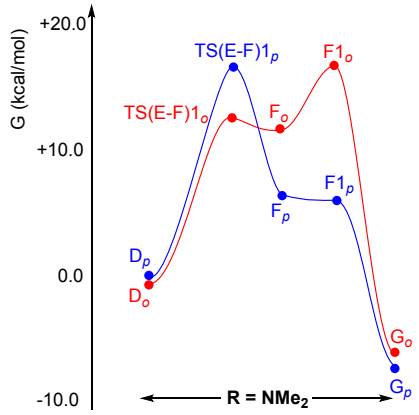

Figure 8. Computed free energy profile (kcal/mol) for the *ortho*- (red) and *para*-cyclometalation reactions (blue) of **L2-NMe$_2$** at $[Ir(OAc)_2Cp^*]$.

Discussion

This study has highlighted that completely opposite selectivities are possible in the cyclometalation reactions of *para*- and *meta*-substituted 1-phenylpyrazoles at $[MCl_2Cp^*]_2$ dimers (M = Rh and Ir) depending on whether the reactions are run under kinetic or thermodynamic control. In the kinetic regime electron donating groups accelerate the reaction, whereas under thermodynamic control electron withdrawing groups are favored. Assigning the mechanism for the current cyclometalation reactions on the basis of substituent electronic effects alone would therefore lead to a different answer depending on whether the system was under kinetic or thermodynamic control. However, under both circumstances here the mechanism must be the same. Thus a single mechanism may favor *either* electron donating groups *or* electron withdrawing groups based on the reaction conditions. We believe that this possibility has so far been overlooked.

With *meta*-substituted ligands **L2-R** most reactions proceed with *para* selectivity and it is only with **L2-F** that the *ortho* isomer is favored both kinetically and thermodynamically. The formation of *ortho*-cyclometalated products in the reactions of fluorinated dimethylbenzylamines at $[Pd(OAc)_2]$ has previously been taken as evidence for an AMLA mechanism rather than S_EAr.[34] The *para*-selectivity is predominantly steric in origin, however, the observation of *ortho*-H/D exchange with some **L2-R** ligands reveals an unexpectedly accessible C–H activation *ortho* to the substituent R. Indeed, *ortho*-C–H activation can even be faster than *para*-C–H activation, as seen in the greater amount of *ortho*-deuteration observed for **L2-NMe$_2$** at Ir and **L2-OMe** at Rh. A similar example was previously noted by Fagnou and coworkers.[46] Our calculations show that with bulky R groups loss of HOAc after *ortho*-C–H activation can be difficult due to steric effects in the 16e intermediates **F1$_o$** and similar steric effects can also disfavor the *ortho*-cyclometalated products **G$_o$**. Thus, as suggested by others, the *o:p* selectivity is steric in origin; however, we have now shown that this steric effect only has a significant impact *after* the C–H activation step.

For the current system, NBO charge distributions were analysed for stationary points along the computed pathways for the *para*-C–H activation of **L2-NMe$_2$** and **L2-NO$_2$** at both Rh and Ir (see Figures S6-11). These indicate the major change to be a polarization of the C–H bond undergoing activation. In addition, only very minor changes are computed for the C–C distances around the activating arene ring.[31] There is therefore no evidence for a Wheland intermediate (i.e. an S_EAr process). These reactions therefore adhere to the AMLA paradigm whereby the ambiphilic combination of a Lewis acidic (i.e. electrophilic) metal center and a chelating base act synergically to cleave the C–H bond. We have previously discussed the similarity of AMLA and CMD and our current results are consistent with our earlier work[9-10,35] and with the thorough analysis of the AMLA/CMD process recently provided by Nielsen and coworkers.[56]

In the context of previous work on mechanisms of carboxylate-assisted C–H activation, Fagnou and Gorelsky showed that the reactions of a wide range of (hetero)aromatic substrates were accelerated (relative to benzene) with more electron-deficient *and* more electron-rich substrates.[29] They showed a CMD mechanism was relevant for all these substrates and rationalized the reactivity patterns in terms of a kinetic effect (see Figure 1). Our present study shows that opposite substituent effects are also possible *in a single reaction*, depending on whether the reaction is under kinetic or thermodynamic control. Hence, relying on electronic substituent effects to assign the mechanism of C–H activation is potentially dangerous. If electron withdrawing substituents react faster, this provides good evidence for an AMLA/CMD mechanism, and in such cases S_EAr is clearly not possible. On the other hand, if a reaction is promoted by electron donating substituents (or with more electron rich substrates) then it does not necessarily mean that it is proceeding via an S_EAr mechanism and, as seen here, AMLA/CMD must still be considered as a possibility.

BIES has sometimes been proposed to describe an electrophilic type mechanism that occurs in the presence of an internal base and is signaled by substrates with electron donating groups reacting faster.[18-20] However our study demonstrates that such reactions can proceed via AMLA/CMD. We therefore suggest that AMLA/CMD and BIES are in fact essentially all the same mechanism, especially when CMD also features an internal base.[55]

In terms of the broader issue of interpreting the nature of a C–H activation within a C–H functionalization catalytic cycle, the relevance of any substituent effect on the overall rate will firstly depend on the identity of the rate-determining process. If this does not involve C–H bond cleavage then a substituent effect may not inform on the nature of the C–H activation. This situation has many parallels with the interpretation of k_H/k_D kinetic isotope effects (KIEs) provided by Hartwig.[57] It is also worth noting that 'C–H activation' may itself involve several steps, including co-ordination of the ligand to the metal, possible formation of a cation by loss of acetate, C–H bond cleavage and then HOAc substitution by another ligand. The actual C–H bond cleavage step may not necessarily be the most difficult of these processes and so may not be rate-limiting. In addition we have shown that even where the overall C–H activation process is likely to be rate limiting, the rate-limiting transition state may not involve significant lengthening or the C–H bond meaning that a significant k_H/k_D KIEs is not observed.[58] This situation arises where the transition state corresponds to the κ^2- κ^1-displacement of acetate which proceeds with minimal C–H bond elongation. Such cases could be viewed as a very early transition state for which a significant k_H/k_D KIE would not be expected.

Non-rate-limiting C–H activation can, however, be selectivity determining and so reflect a substituent effect. Our results show that the interpretation of selectivity effects will depend on whether C–H activation is reversible within the catalytic cycle (thermodynamic control) or irreversible (kinetic control). Indeed, this may depend not only on the reaction conditions but also on the activation barriers for the subsequent steps. In many cases C–H activation with Cp*Rh is reversible in the absence of a coupling partner, but apparently irreversible (based on H/D exchange) in the presence of such a substrate. The latter situation pertains when the transition state energy for the next step is lower than for C–H activation. The context of the C–H activation process within the catalytic cycle must therefore be understood if appropriate conclusions are to be made. Returning to the current work, we have described a system where the selectivities differ depending on whether kinetic or thermodynamic control is in play. In other cases the selectivity may not change upon varying the reaction conditions and other factors may dominate the observed selectivity, including the charge of the catalyst, cationic (as here) or neutral as in direct arylation studied by Fagnou, or charge of a directing group, neutral here but sometimes anionic.)

Conclusions

We have reported here a series of acetate-assisted cyclometalations of *meta*- and *para*-substituted 1-phenylpyrazoles at $[MCl_2Cp^*]_2$ dimers (M = Ir, Rh). Electronic substituent effects depend on whether the reaction is under kinetic or thermodynamic control. Under kinetic control, the relative rates of cyclometalation correlate well with the Hammett parameters of the substituents, with faster reactions observed with electron donating substituents. However, under thermodynamic control the products with electron withdrawing substituents are preferred. Despite these

apparently conflicting selectivities all these reactions proceed by an AMLA/CMD C–H activation mechanism and the observed selectivity depends on the substituent, the metal and the reaction conditions.

Our results show that attempting to assign the mechanism of a carboxylate-assisted C–H activation through the use of a small number of competition reactions involving differently substituted substrates is potentially dangerous without further information on whether kinetic or thermodynamic control is involved. For catalysis this may also be dependent on the transition state energy for the next steps in the cycle. If such a reaction is promoted by electron deficient substrates it is likely to be proceeding by an AMLA/CMD mechanism. However, the situation is less clear if electron donating substituents promote the reaction: such processes are certainly "electrophilic", in that they involve an electron deficient metal center, but this should not be taken to mean they necessarily involve an S_EAr mechanism. If such reactions work significantly better with carboxylate bases, and the nature of the carboxylate has an effect on the C–H activation step, then it is likely that an AMLA/CMD/BIES mechanism is involved. In our opinion AMLA/CMD and BIES are essentially all the same mechanism.

H/D exchange reactions highlight a surprising kinetic accessibility for *ortho*-C-H activation in a number of *meta*-substituted 1-phenylpyrazoles. Analysis of these reactions shows that in these half-sandwich complexes steric effects have the largest impact after the C–H activation step. In particular HOAc dissociation is significantly disfavored due to the high energy of the 16e intermediates formed. HOAc dissociation can therefore be a kinetically relevant process that may need to be taken into account when considering the mechanism of C–H activation, whether as a stoichiometric process or within a catalytic cycle.

ASSOCIATED CONTENT

Supporting Information. Crystallographic data (CIF), full experimental details, NMR spectra, and details of all computed reaction profiles, energies, NBO analyses and Cartesian coordinates. CCDC 1897016-1897025 contain complete crystallographic data for this paper and these data can be obtained free of charge from The Cambridge Crystallographic Data Centre via http://www.ccdc.cam.ac.uk/pages/Home.aspx. The Supporting Information is available free of charge via the Internet at http://pubs.acs.org.

AUTHOR INFORMATION

Corresponding Author

*dld3@leicester.ac.uk
*s.a.macgregor@hw.ac.uk

Present Addresses

‡ Department of Chemistry, College of Education for Pure Sciences, University of Basrah, Basrah, Iraq.
†Department of Chemistry, University of Bath, Claverton Down, Bath BA2 7AY, United Kingdom

ACKNOWLEDGMENT

We thank the EPSRC for financial support through awards EP/J002712/1 and EP/J021911/1 (S.A.M.) and EP/J002917/1 and EP/J021709/1 (D.L.D.) and EUCOST Action CA15106 "C−H Activation in Organic Synthesis (CHAOS)". RAA thanks the Iraq government for a scholarship.

REFERENCES

(1) Song, G.; Wang, F.; Li, X., C-C, C-O and C-N bond formation via rhodium(iii)-catalyzed oxidative C-H activation. *Chem. Soc. Rev.* **2012**, *41*, 3651-3678.
(2) Gensch, T.; Hopkinson, M. N.; Glorius, F.; Wencel-Delord, J., Mild metal-catalyzed C-H activation: examples and concepts. *Chem. Soc. Rev.* **2016**, *45*, 2900-2936.
(3) Ackermann, L., Carboxylate-Assisted Transition-Metal-Catalyzed C−H Bond Functionalizations: Mechanism and Scope. *Chem. Rev.* **2011**, *111*, 1315-1345.
(4) Arockiam, P. B.; Bruneau, C.; Dixneuf, P. H., Ruthenium(II)-Catalyzed C–H Bond Activation and Functionalization. *Chem. Rev.* **2012**, *112*, 5879-5918.
(5) Smith, M. B.; March, J. In *Advanced Organic Chemistry*; Wiley-VCH Hoboken: 2007, p Chapter 11.
(6) García-Cuadrado, D.; Braga, A. A. C.; Maseras, F.; Echavarren, A. M., Proton abstraction mechanism for the palladium-catalyzed intramolecular arylation. *J. Am. Chem. Soc.* **2006**, *128*, 1066-1067.
(7) Lafrance, M.; Rowley, C. N.; Woo, T. K.; Fagnou, K., Catalytic intermolecular direct arylation of perfluorobenzenes. *J. Am. Chem. Soc.* **2006**, *128*, 8754-8756.
(8) Lapointe, D.; Fagnou, K., Overview of the Mechanistic Work on the Concerted Metallation-Deprotonation Pathway. *Chem. Lett.* **2010**, *39*, 1119-1126.
(9) Boutadla, Y.; Davies, D. L.; Macgregor, S. A.; Poblador-Bahamonde, A. I., Mechanisms of C-H bond activation: rich synergy between computation and experiment. *Dalton Trans.* **2009**, 5820-5831.
(10) Davies, D. L.; Donald, S. M. A.; Macgregor, S. A., Computational Study of the Mechanism of Cyclometallation by Palladium Acetate. *J. Am. Chem. Soc.* **2005**, *127*, 13754-13755.
(11) Ess, D. H.; Bischof, S. M.; Oxgaard, J.; Periana, R. A.; Goddard, W. A., Transition State Energy Decomposition Study of Acetate-Assisted and Internal Electrophilic Substitution C−H Bond Activation by (acac-O,O)2Ir(X) Complexes (X = CH3COO, OH). *Organometallics* **2008**, *27*, 6440-6445.
(12) Li, B.; Xu, H.; Wang, H.; Wang, B., Rhodium-Catalyzed Annulation of Tertiary Aniline N-Oxides to N-Alkylindoles: Regioselective C–H Activation, Oxygen-Atom Transfer, and N-Dealkylative Cyclization. *ACS Catal* **2016**, *6*, 3856-3862.
(13) Thirunavukkarasu, V. S.; Raghuvanshi, K.; Ackermann, L., Expedient C–H Amidations of Heteroaryl Arenes Catalyzed by Versatile Ruthenium(II) Catalysts. *Org. Lett.* **2013**, *15*, 3286-3289.
(14) Huang, X.; Huang, J.; Du, C.; Zhang, X.; Song, F.; You, J., N-Oxide as a Traceless Oxidizing Directing Group: Mild Rhodium(III)-Catalyzed C-H Olefination for the Synthesis of ortho-Alkenylated Tertiary Anilines. *Angew. Chem., Int. Ed.* **2013**, *52*, 12970-12974.
(15) Guo, X.; Han, J.; Liu, Y.; Qin, M.; Zhang, X.; Chen, B., Synthesis of 2,3-Disubstituted NH Indoles via Rhodium(III)-Catalyzed C–H Activation of Arylnitrones and Coupling with Diazo Compounds. *J. Org. Chem.* **2017**, *82*, 11505-11511.
(16) Tan, E.; Quinonero, O.; Elena de Orbe, M.; Echavarren, A. M., Broad-Scope Rh-Catalyzed Inverse-Sonogashira Reaction Directed by Weakly Coordinating Groups. *ACS Catal* **2018**, *8*, 2166-2172.
(17) Originally termed IES see ref 10, the same mechanism has often been referred to as base assisted internal electrophilic substituion (BIES).
(18) Debbarma, S.; Bera, S. S.; Maji, M. S., Cp*Rh(III)-Catalyzed Low Temperature C–H Allylation of N-Aryl-trichloro Acetimidamide. *J. Org. Chem.* **2016**, *81*, 11716-11725.

(19) Ma, W.; Mei, R.; Tenti, G.; Ackermann, L., Ruthenium(II)-Catalyzed Oxidative C-H Alkenylations of Sulfonic Acids, Sulfonyl Chlorides and Sulfonamides. *Chem. Eur. J.* **2014**, *20*, 15248-15251.

(20) Mei, R.; Zhang, S.-K.; Ackermann, L., Ruthenium(II)-Catalyzed C–H Alkynylation of Weakly Coordinating Benzoic Acids. *Org. Lett.* **2017**, *19*, 3171-3174.

(21) Lv, H.; Shi, J.; Huang, J.; Zhang, C.; Yi, W., Rhodium(iii)-catalyzed and MeOH-involved regioselective mono-alkenylation of N-arylureas with acrylates. *Org. Biomol. Chem.* **2017**, *15*, 7088-7092.

(22) Yu, D.-G.; de Azambuja, F.; Glorius, F., α-MsO/TsO/Cl Ketones as Oxidized Alkyne Equivalents: Redox-Neutral Rhodium(III)-Catalyzed C-H Activation for the Synthesis of N-Heterocycles. *Angew. Chem., Int. Ed.* **2014**, *53*, 2754-2758.

(23) Semwal, S.; Ghorai, D.; Choudhury, J., Wingtip-Dictated Cyclometalation of N-Heterocyclic Carbene Ligand Framework and Its Implication toward Tunable Catalytic Activity. *Organometallics* **2014**, *33*, 7118-7124.

(24) Ackermann, L.; Lygin, A. V.; Hofmann, N., Ruthenium-Catalyzed Oxidative Annulation by Cleavage of C-H/N-H Bonds. *Angew. Chem., Int. Ed.* **2011**, *50*, 6379-6382.

(25) Ma, W.; Graczyk, K.; Ackermann, L., Ruthenium-Catalyzed Alkyne Annulations with Substituted 1H-Pyrazoles by C–H/N–H Bond Functionalizations. *Org. Lett.* **2012**, *14*, 6318-6321.

(26) Ryabov, A. D.; Sakodinskaya, I. K.; Yatsimirsky, A. K., Kinetics and Mechanism of Ortho-Palladation of Ring-Substituted *N,N*-Dimethylbenzylamines. *J. Chem. Soc., Dalton Trans.* **1985**, 2629-2638.

(27) Váňa, J.; Terencio, T.; Petrović, V.; Tischler, O.; Novák, Z.; Roithová, J., Palladium-Catalyzed C–H Activation: Mass Spectrometric Approach to Reaction Kinetics in Solution. *Organometallics* **2017**, *36*, 2072-2080.

(28) subsequently an alternative process involving bicarbonate as an external base was also shown to be competitive. García-Cuadrado, D.; de Mendoza, P.; Braga, A. A. C.; Maseras, F.; Echavarren, A. M., Proton-Abstraction Mechanism in the Palladium-Catalyzed Intramolecular Arylation: Substituent Effects. J. Am. Chem. Soc. 2007, 129 (21), 6880-6886.

(29) Gorelsky, S. I.; Lapointe, D.; Fagnou, K., Analysis of the Palladium-Catalyzed (Aromatic)C-H Bond Metalation-Deprotonation Mechanism Spanning the Entire Spectrum of Arenes. *J. Org. Chem.* **2012**, *77*, 658-668.

(30) Gorelsky, S. I.; Lapointe, D.; Fagnou, K., Analysis of the Concerted Metalation-Deprotonation Mechanism in Palladium-Catalyzed Direct Arylation Across a Broad Range of Aromatic Substrates. *J. Am. Chem. Soc.* **2008**, *130*, 10848-10849.

(31) Gorelsky, S. I., Origins of regioselectivity of the palladium-catalyzed (aromatic)CH bond metalation–deprotonation. *Coord. Chem. Rev.* **2013**, *257*, 153-164.

(32) Davies, D. L.; Macgregor, S. A.; McMullin, C. L., Computational Studies of Carboxylate-Assisted C–H Activation and Functionalization at Group 8–10 Transition Metal Centers. *Chem. Rev.* **2017**.

(33) Petit, A.; Flygare, J.; Miller, A. T.; Winkel, G.; Ess, D. H., Transition-State Metal Aryl Bond Stability Determines Regioselectivity in Palladium Acetate Mediated C-H Bond Activation of Heteroarenes. *Org. Lett.* **2012**, *14*, 3680-3683.

(34) Milani, J.; Pridmore, N. E.; Whitwood, A. C.; Fairlamb, I. J. S.; Perutz, R. N., The Role of Fluorine Substituents in the Regioselectivity of Intramolecular C–H Bond Functionalization of Benzylamines at Palladium(II). *Organometallics* **2015**, *34*, 4376-4386.

(35) Davies, D. L.; Donald, S. M. A.; Al-Duaij, O.; Macgregor, S. A.; Pölleth, M., Electrophilic C−H Activation at {Cp*Ir}: Ancillary-Ligand Control of the Mechanism of C−H Activation. *J. Am. Chem. Soc.* **2006**, *128*, 4210-4211.

(36) Li, L.; Brennessel, W. W.; Jones, W. D., C−H Activation of Phenyl Imines and 2-Phenylpyridines with [Cp*MCl2]2 (M = Ir, Rh): Regioselectivity, Kinetics, and Mechanism. *Organometallics* **2009**, *28*, 3492-3500.

(37) Broeckx, L. E. E.; Güven, S.; Heutz, F. J. L.; Lutz, M.; Vogt, D.; Müller, C., Cyclometalation of Aryl-Substituted Phosphinines through C□H-Bond Activation: A Mechanistic Investigation. *Chem. Eur. J.* **2013**, *19*, 13087-13098.

(38) Li, J.; Hu, W.; Peng, Y.; Zhang, Y.; Li, J.; Zheng, W., Theoretical Study on Iridacycle and Rhodacycle Formation via C–H Activation of Phenyl Imines. *Organometallics* **2014**, *33*, 2150-2159.

(39) Carr, K. J. T.; Macgregor, S. A.; Davies, D. L.; Singh, K.; Villa-Marcos, B., Metal control of selectivity in acetate-assisted C-H bond activation: An experimental and computational study of heterocyclic, vinylic and phenylic C(sp)-H bonds at Ir and Rh. *Chem. Sci.* **2014**, *5*, 2340-2346.

(40) Li, X.; Zhao, M., Rhodium(III)-Catalyzed Oxidative Coupling of 5-Aryl-1H-pyrazoles with Alkynes and Acrylates. *J. Org. Chem.* **2011**, *76*, 8530-8536.

(41) Lian, Y.; Bergman, R. G.; Lavis, L. D.; Ellman, J. A., Rhodium(III)-Catalyzed Indazole Synthesis by C–H Bond Functionalization and Cyclative Capture. *J. Am. Chem. Soc.* **2013**, *135*, 7122-7125.

(42) Muralirajan, K.; Cheng, C.-H., Rhodium(III)-Catalyzed Synthesis of Cinnolinium Salts from Azobenzenes and Alkynes: Application to the Synthesis of Indoles and Cinnolines. *Chemistry – A European Journal* **2013**, *19*, 6198-6202.

(43) Oh, Y.; Han, S. H.; Mishra, N. K.; De, U.; Lee, J.; Kim, H. S.; Jung, Y. H.; Kim, I. S., Synthesis and Anticancer Evaluation of 2,3-Disubstituted Indoles Derived from Azobenzenes and Internal Olefins. *Eur. J. Org. Chem.* **2017**, *2017*, 6265-6273.

(44) Chen, X.; Zheng, G.; Song, G.; Li, X., Rhodium(III)-Catalyzed Synthesis of Cinnolinium Salts from Azobenzenes and Diazo Compounds. *Adv. Synth. Catal.* **2018**, *360*, 2836-2842.

(45) Hyster, T. K.; Rovis, T., Rhodium-Catalyzed Oxidative Cycloaddition of Benzamides and Alkynes via C−H/N−H Activation. *J. Am. Chem. Soc.* **2010**, *132*, 10565-10569.

(46) Stuart, D. R.; Bertrand-Laperle, M.; Burgess, K. M. N.; Fagnou, K., Indole Synthesis via Rhodium Catalyzed Oxidative Coupling of Acetanilides and Internal Alkynes. *J. Am. Chem. Soc.* **2008**, *130*, 16474-16475.

(47) Frasco, D. A.; Mukherjee, S.; Sommer, R. D.; Perry, C. M.; Lambic, N. S.; Abboud, K. A.; Jakubikova, E.; Ison, E. A., Nondirected C–H Activation of Arenes with Cp*Ir(III) Acetate Complexes: An Experimental and Computational Study. *Organometallics* **2016**, *35*, 2435-2445.

(48) Simonetti, M.; Kuniyil, R.; Macgregor, S. A.; Larrosa, I., Benzoate Cyclometalation Enables Oxidative Addition of Haloarenes at a Ru(II) Center. *J. Am. Chem. Soc.* **2018**, *140*, 11836-11847.

(49) Boutadla, Y.; Davies, D. L.; Al-Duaij, O.; Fawcett, J.; Jones, R. C.; Singh, K., Alkyne insertion into cyclometallated pyrazole and imine complexes of iridium, rhodium and ruthenium; relevance to catalytic formation of carbo- and heterocycles. *Dalton Trans.* **2010**, *39*, 10447-10457.

(50) It was clear from the experiments carried out that the more electron donating substrates gave more H/D exchange and some of the more electron withdrawing ligands gave no exchange after a few weeks at room temperature hence it was not felt necessary to test every ligand. .

(51) The relative rate for formation of the para isomer has been multiplied by 2 since two equivalent sites are available in formation of the meta complexes.

(52) experimentally a 4:1 DCM:MeOH ratio was employed to ensure complete product solubility and so solvent effects were assess by re-running the solvent correction with MeOH. The ligand dissociation steps (D to E, F to F1 and F1 to G) were most affected, but overall trends in the computed barriers and thermodynamics were very similar in both solvents. Data computed in MeOH are provided in Tables S9 (Ir) and S10 (Rh) in the ESI.

(53) Davies, D. L.; Ellul, C. E.; Macgregor, S. A.; McMullin, C. L.; Singh, K., Experimental and DFT Studies Explain Solvent Control of C–H Activation and Product Selectivity in the Rh(III)-Catalyzed Formation of Neutral and Cationic Heterocycles. *J. Am. Chem. Soc.* **2015**, *137*, 9659-9669.

(54) The reaction of **L2-NMe$_2$** at Rh involves an additional intermediate at +11.3 kcal/mol that links directly to **TS(E-F)2$_p$**.This has a slightly different orientation of the phenylpyrazole moiety

compared to **Int(E-P)$_p$** and is linked to that structure via a transition state at +13.0 kcal/mol. As this lies below **TS(E-F)2$_p$** at +13.5 kcal/mol it is omitted from Figure 4 for clarity. A similar profile was also seen for **L2-OMe** reacting at Rh (see ESI for full details).

(55) Deprotonation by external base was also considered but was shown to be less accessible (see ESI).

(56) Sajjad, M. A.; Christensen, K. E.; Rees, N. H.; Schwerdtfeger, P.; Harrison, J. A.; Nielson, A. J., Chasing the agostic interaction in ligand assisted cyclometallation reactions of palladium(ii). *Dalton Trans.* **2017**, *46*, 16126-16138.

(57) Simmons, E. M.; Hartwig, J. F., On the Interpretation of Deuterium Kinetic Isotope Effects in C-H Bond Functionalizations by Transition-Metal Complexes. *Angew. Chem., Int. Ed.* **2012**, *51*, 3066-3072.

(58) Algarra, A. G.; Cross, W. B.; Davies, D. L.; Khamker, Q.; Macgregor, S. A.; McMullin, C. L.; Singh, K., Combined Experimental and Computational Investigations of Rhodium- and Ruthenium-Catalyzed C–H Functionalization of Pyrazoles with Alkynes. *J. Org. Chem.* **2014**, *79*, 1954-1970.

Authors are required to submit a graphic entry for the Table of Contents (TOC) that, in conjunction with the manuscript title, should give the reader a representative idea of one of the following: A key structure, reaction, equation, concept, or theorem, etc., that is discussed in the manuscript. Consult the journal's Instructions for Authors for TOC graphic specifications.

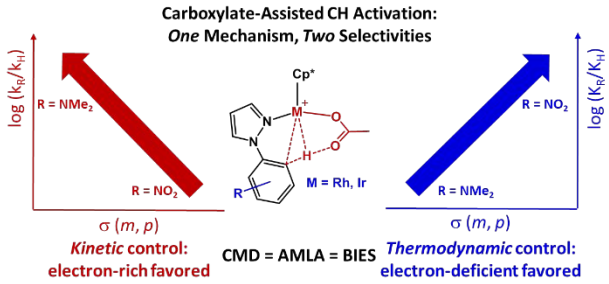

Insert Table of Contents artwork here

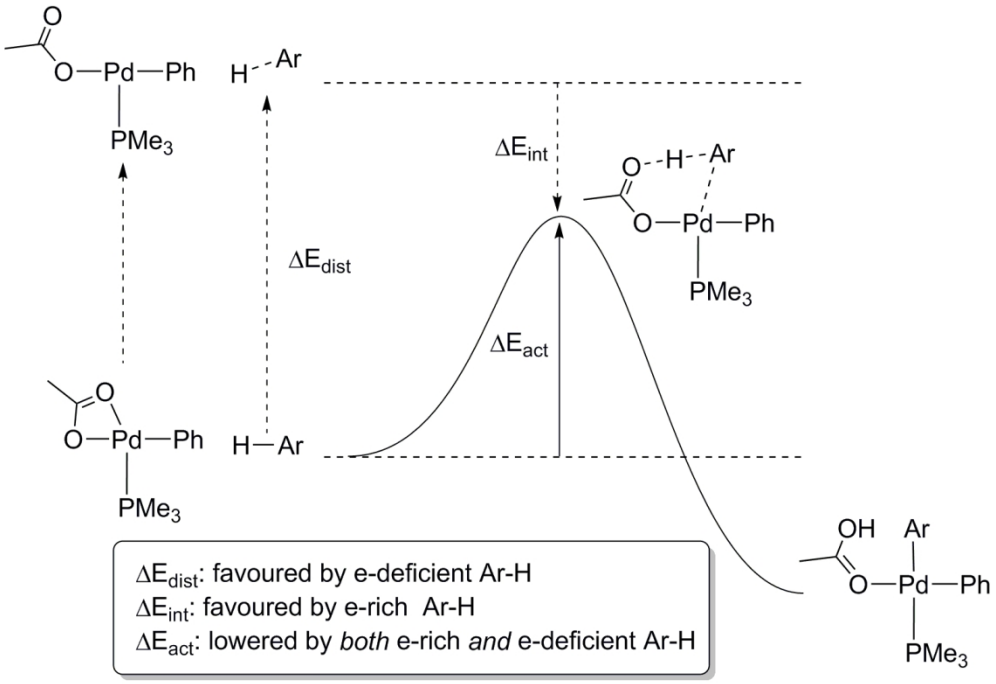

Figure 1. The distortion-interaction model applied to C-H activation of (hetero)aromatic substrates, Ar-H, at [Pd(OAc)Ph(PMe_3)]. Adapted from reference [29].

137x94mm (300 x 300 DPI)

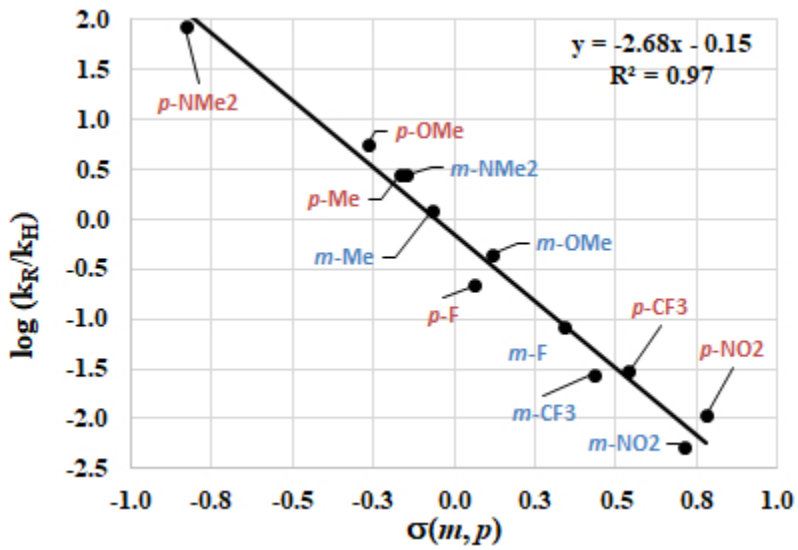

Figure 2. Hammett plot of log (kR/k_H) for formation of *meta*-**1-R** and *para*-substituted **3-R** complexes of Ir against σ_m and σ_p.

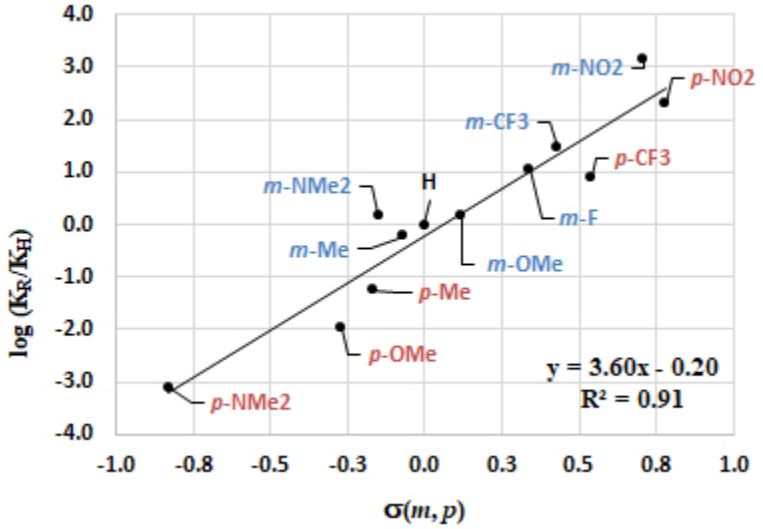

Figure 3. Plot of $\ln(K_R/K_H)$ for formation of *meta* **1a-R** and *para*-substituted **3a-R** complexes of Ir against σ_m and σ_p.

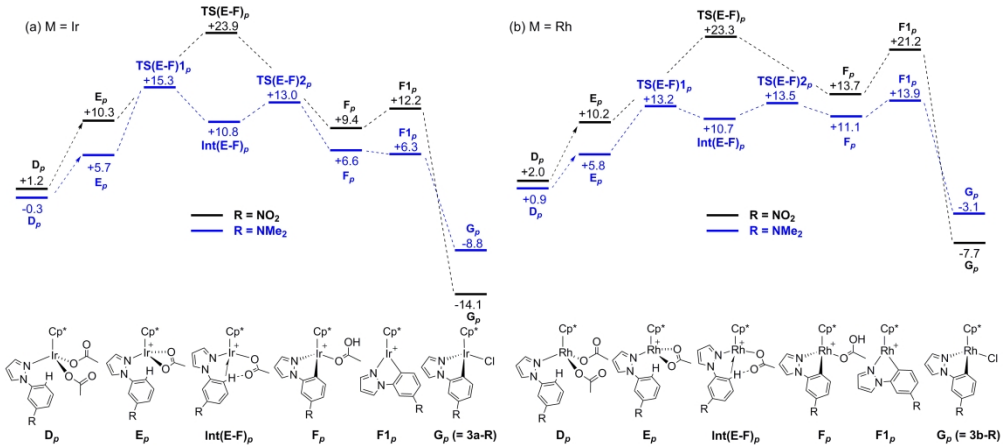

Figure 4. Computed free energy profiles (kcal/mol) for the reactions of **L2-NMe$_2$** (blue) and **L2-NO$_2$** (black) at (a) $[IrCl_2Cp^*]_2$ and (b) $[RhCl_2Cp^*]_2$. Free energies are quoted relative to $[M(OAc)_2Cp^*]$ (**C**) and the free ligand set to 0.0 kcal/mol.

320x142mm (300 x 300 DPI)

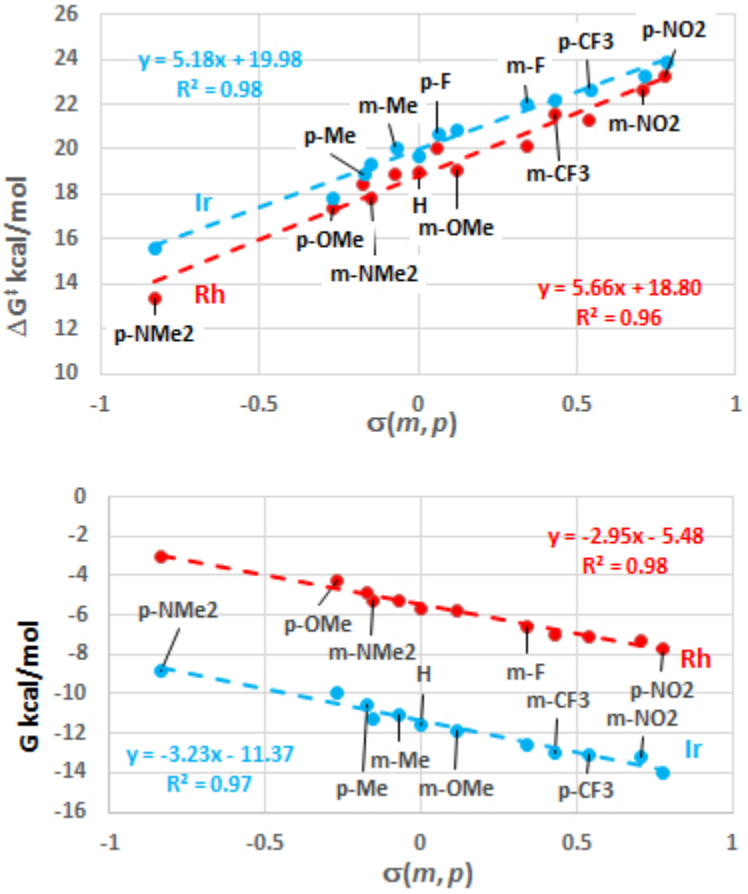

Figure 5. Plots of computed values of $\Delta G^{\ddagger}$ and ΔG (kcal/mol) against σ_m and σ_p Hammett constants for the reactions of **L1-R** and **L2-R** to form **1a/b-R** and **3a/b-R**

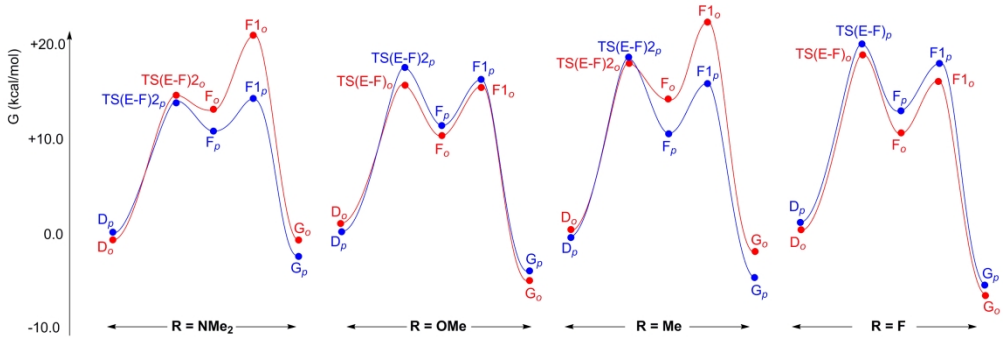

Figure 6. Computed free energy profiles (kcal/mol) for the *ortho*- (red) and *para*-cyclometalation reactions (blue) of **L2-R** at [Rh(OAc)$_2$Cp*].

251x85mm (300 x 300 DPI)

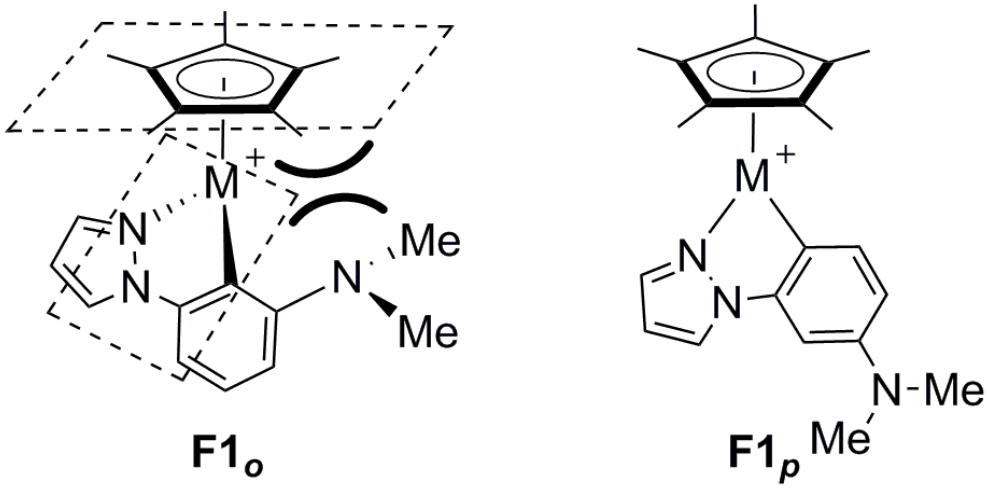

Figure 7. Schematic structures of **F1**$_o$ and **F1**$_p$ illustrating steric hindrance in **F1**$_o$.

78x39mm (300 x 300 DPI)

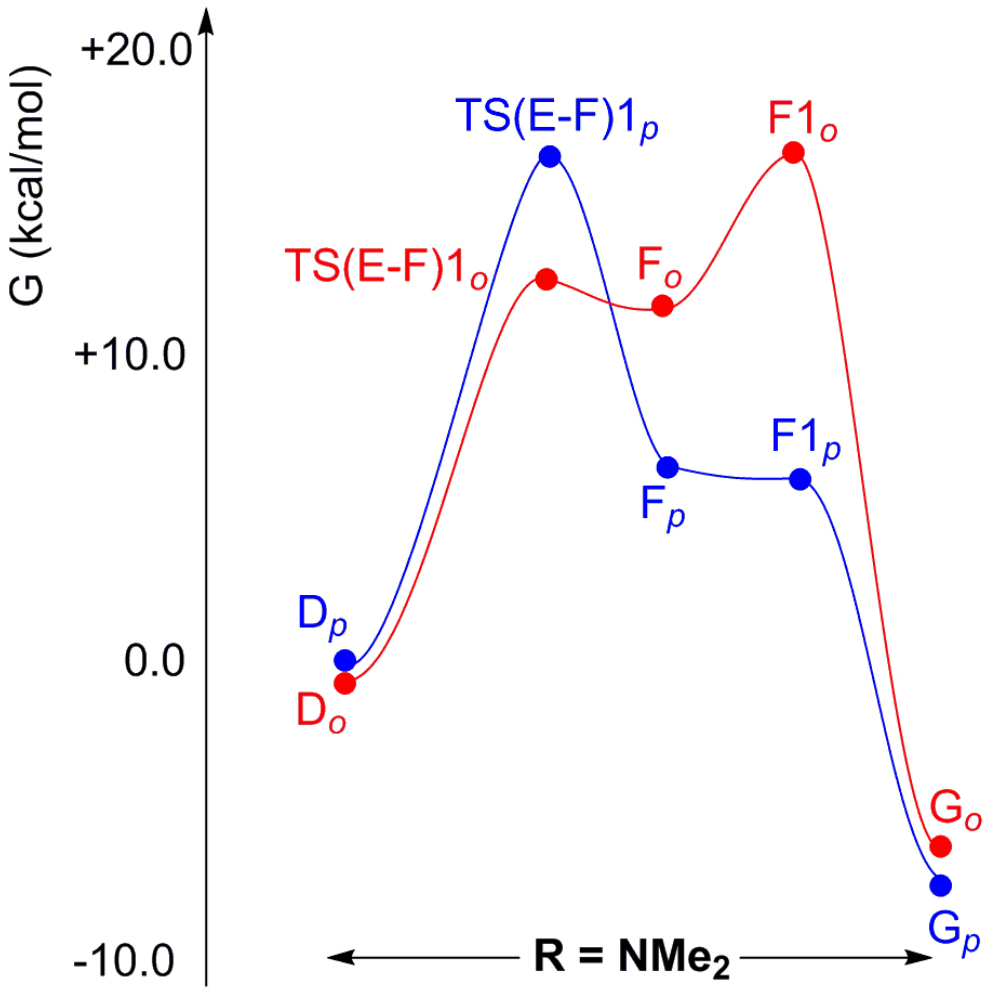

Figure 8. Computed free energy profile (kcal/mol) for the *ortho*- (red) and *para*-cyclometalation reactions (blue) of **L2-NMe$_2$** at [Ir(OAc)$_2$Cp*]

78x78mm (300 x 300 DPI)

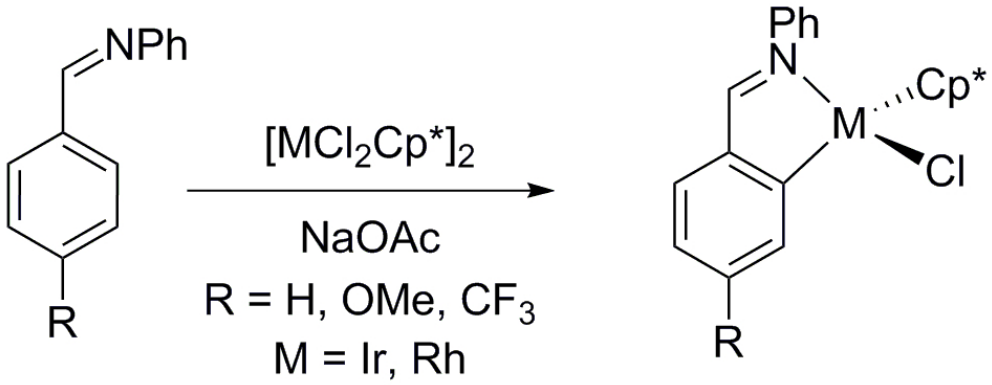

Scheme 1. Formation of cyclometalated imines.[36]

80x32mm (300 x 300 DPI)

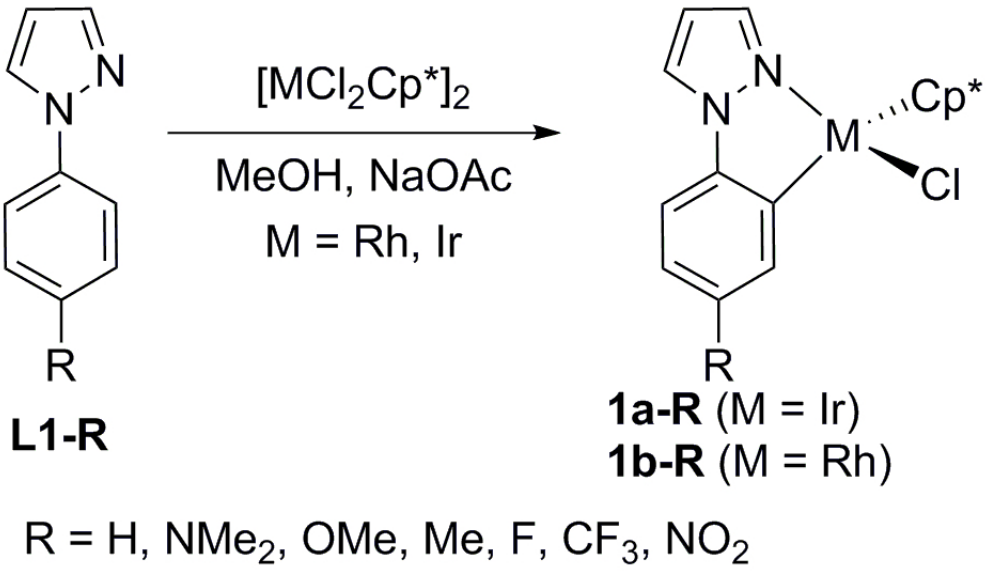

Scheme 2. Formation of *meta*-substituted cyclometalated complexes **1a-R** (M = Ir) and **1b-R** (M = Rh).

79x45mm (300 x 300 DPI)

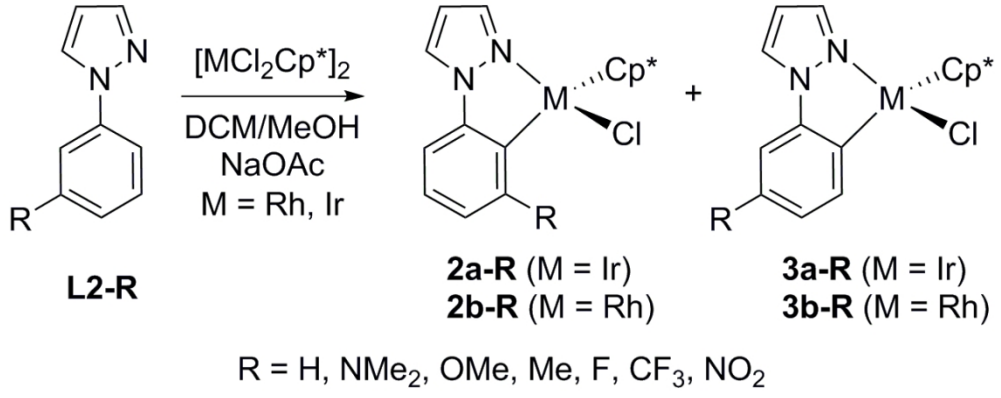

Scheme 3. Formation of *ortho* and/or *para*-substituted cyclometalated complexes **2a-R** and **3a-R** (M = Ir) and **2b-R** and **3b-R** (M = Rh).

108x43mm (300 x 300 DPI)

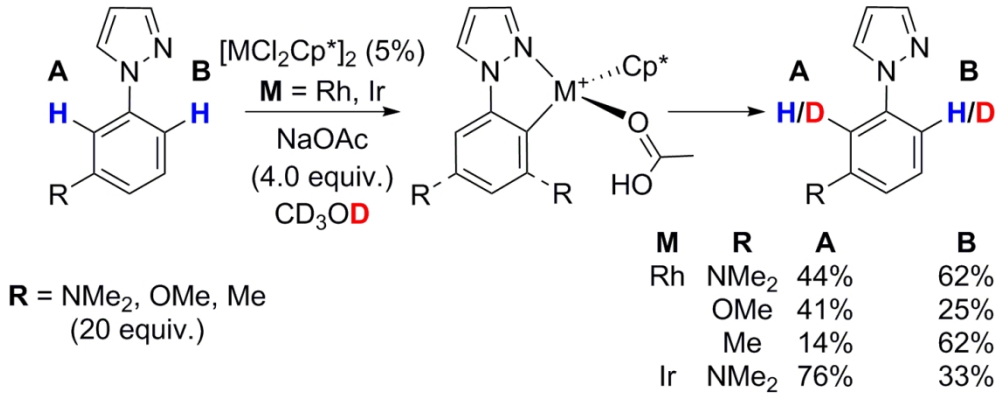

Scheme 4. Room temperature H/D exchange for *meta*-substituted ligands at sites A and B

123x49mm (300 x 300 DPI)

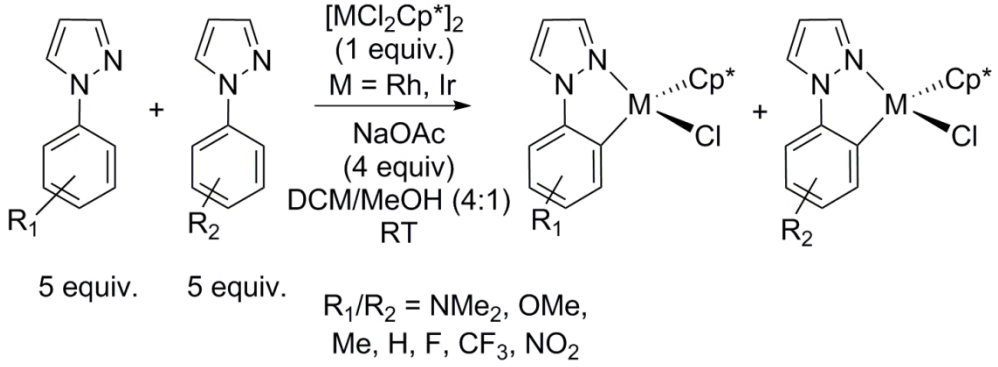

Scheme 5. Competition experiments; for results of individual experiments see ESI.

122x46mm (300 x 300 DPI)